

Photoproton decay of the ^{31}P giant resonance

E. Kerkhove,* H. Ferdinande, P. Van Otten, D. Ryckbosch,
R. Van de Vyver, P. Berkvens, and E. Van Camp
Laboratorium voor Kernfysica, Rijksuniversiteit Gent, B-9000 Gent, Belgium

A. Aksoy

Faculty of Engineering of Sakarya, Istanbul Technical University, Adapazari, Turkey

(Received 2 July 1984)

The $^{31}\text{P}(\gamma, p)^{30}\text{Si}$ reaction was studied at seven angles for nine bremsstrahlung end point energies varying from 17 to 25 MeV in 1 MeV steps. Absolute (γ, p_0) and (γ, p_1) angular cross sections for ^{31}P in the excitation energy interval between 14.6 and 25 MeV were extracted and angular distribution factors were deduced by fitting a sum of Legendre polynomials to the data. Absolute cross sections for various other photoproton reaction channels were determined using an artificially constructed pseudo-monoenergetic photon spectrum. The total (γ, p) cross section was evaluated up to 24 MeV excitation energy. About 53% of this cross section is due to a direct-semidirect reaction mechanism. The angular distribution factors in the (γ, p_0) channel were used to estimate the contribution of $E2$ photon absorption in this channel. It was found that between 48% and 63% of the isoscalar $E2$ energy-weighted sum rule is exhausted by this (γ, p_0) channel.

I. INTRODUCTION

Since the start of photonuclear physics, much interest has centered on the light $(2s-1d)$ shell nuclei. The giant electric dipole resonance (GDR) for these nuclides is known to be considerably fragmented;¹ the self-conjugate even-even nuclei in this region have been investigated in detail and show more structure than the nearby odd-mass ones. As the (γ, p) reaction for these nuclei frequently provides more than half of the photoabsorption cross section (which is the case for ^{31}P), the photoproton channel is an important study tool.

The experiments reported in this paper link up with recent investigations of other $4N+3$ nuclei belonging to the $(2s-1d)$ shell, for which a diverse range of features was observed. Effects due to configurational splitting resulting from inner and outer shell excitation, isospin splitting, and static deformation have been observed or postulated for these nuclides. In fact, ^{19}F (with $N=4$) has been studied recently in this laboratory,² while ^{27}Al (for which $N=6$) was thoroughly investigated by Ishkhanov *et al.*³ and by Ryan *et al.*⁴

The ^{31}P photonuclear $E1$ giant resonance has been investigated extensively by (γ, n) studies,^{5,6} by an (e, p) experiment,⁷ and via the inverse (p, γ) reaction⁸ and also by $(\gamma, x\gamma')$ measurements.⁹ The present work describes a measurement of the angular photoproton spectra from ^{31}P . From these spectra absolute ^{31}P partial photoproton cross sections leading to specific states or groups of states in the residual nucleus ^{30}Si are deduced, since these "states" are well separated in energy (see Sec. III C).

II. EXPERIMENTAL PROCEDURE AND DATA ANALYSIS

The bremsstrahlung facility of the 70 MeV linear electron accelerator of Ghent State University was used as the

photon source in this work. The target consisted of natural red phosphorus (with a purity in excess of 99%) deposited on both sides of a Au foil of thickness $0.5\ \mu\text{m}$. The total thickness of the ^{31}P material was $4.6\ \text{mg cm}^{-2}$. Photoproton spectra were measured simultaneously at seven angles θ between 37° and 143° by means of uncooled Si(Li) detectors. The experimental setup was described in detail in a previous paper.¹⁰ The bremsstrahlung end point energy was stepped in 1 MeV intervals between 17 and 25 MeV. The experimental energy resolution was to a large extent determined by the energy loss of the photoprotons in the target material and varied between 250 and 100 keV for the proton kinetic energies $E_{k,p}$ ranging from 6 up to 20 MeV. The proton energy calibration procedure, the correction for energy loss in the target, and the use of the Schiff bremsstrahlung spectrum near the tip region corrected for energy loss of the electrons in the radiator were discussed in a previous paper.¹¹

As the first excited state in the residual nucleus ^{30}Si is situated at 2.24 MeV (Fig. 1), it was possible to directly derive the angular (γ, p_0) cross section for the seven angles θ in the energy interval ranging from 14.6 to 24.8 MeV (Fig. 2). After subtraction of the (γ, p_0) contribution from the originally measured (γ, p) spectra, it was also possible to determine the angular (γ, p_1) cross sections, since the energy difference between the first and second excited state in ^{30}Si is about 1.26 MeV; those cross sections are shown in Fig. 3.

A sum of Legendre polynomials was fitted to these angular cross sections in the usual way:

$$\frac{d\sigma}{d\Omega}(\theta, E) = A_0(E) \left[1 + \sum_{\nu=1}^m a_\nu(E) P_\nu(\cos\theta) \right],$$

with the angular distribution factors $a_\nu(E) = A_\nu(E)/A_0(E)$. For the (γ, p_0) cross sections this fitting was performed to the fourth order in the Legendre polynomial,

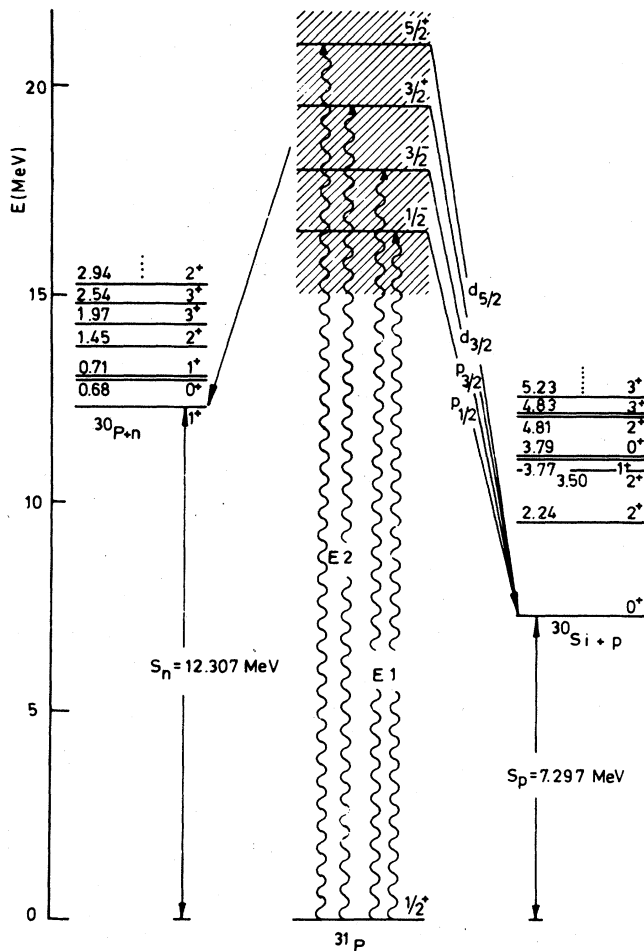


FIG. 1. Energy-level diagram for the (γ,n) and (γ,p) reactions in the case of ^{31}P and schematic representation of $E1$ and $E2$ photon absorption and subsequent p -wave and d -wave, respectively, emission to the ^{30}Si ground state; energy, spin, and parity assignments are given according to Ref. 16.

i.e., $m=4$, while for the (γ,p_i) data $m=2$, due to the much poorer statistics involved, caused by the peeling off technique.

In order to use most of the information contained in the measured proton spectra a nearly monoenergetic photon spectrum was constructed artificially by taking an algebraic sum of suitably normalized bremsstrahlung spectra with consecutive end point energies. The same procedure, with normalization in the same way, was applied to the corresponding photoproton spectra as a function of the proton kinetic energy $E_{k,p}$. This method allows us to determine a spectral, angular photoproton cross section $d^2\sigma/(d\Omega dE_{k,p})$ that corresponds to the above generated quasi-monoenergetic photon flux. Integrated-over-angles photoproton spectral cross sections $d\sigma/dE_{k,p}$ can be produced by the above-mentioned Legendre polynomial fitting procedure. After integration over proton kinetic energy, absolute (γ,p_i) reaction cross sections are obtained for the decay to specific states or groups of states (labeled by $i=0,1,2,\dots$) in the ^{30}Si residual nucleus. This pro-

cedure has been outlined in detail in earlier papers.^{12,13} As the groups of final states in the residual nucleus, which are populated in the (γ,p) process (see Sec. III C), are separated in energy by amounts larger than the bremsstrahlung energy step (1 MeV), it was possible to repeat the subtraction or peeling off procedure, such as was explained above, to extract the (γ,p_i) angular cross sections from the original data and to determine in this way the angular (γ,p_i) cross sections as well. A Legendre polynomial fitting to those angular data was also limited to second order for the same reason as in the (γ,p_i) case and delivers now in an alternative way the absolute (γ,p_i) cross sections for decay to the groups of states $i=2, 3$, and 4.

Finally, in order to also obtain a rough picture of the total $^{31}\text{P}(\gamma,p)$ cross section we subtracted an exponentially decreasing background^{12,13} (originating from low-energy secondary electrons and scattered photons) from the raw individual photoproton spectra and constructed a total (again over-angles-integrated) photoproton yield curve as a function of bremsstrahlung end point energy. It should be noted, however, that in our proton yields only protons with kinetic energy greater than approximately 3 MeV could be used. Applying the Thies analysis method¹⁴ the resulting yield curve was unfolded to a total (γ,p) cross section, which should be considered as a lower limit according to the above-mentioned consideration.

In the following sections we will quote only statistical errors and the error bars presented in all the figures will be statistical in nature only. The total systematic uncertainty is estimated to be of the order of 10%.

III. RESULTS AND DISCUSSION

A. The $^{31}\text{P}(\gamma,p_0)$ cross section

The total integrated-over-angles absolute ground state cross section, which equals $\sigma(E)=4\pi A_0(E)$, and the angular distribution factors a_ν ($\nu=1, \dots, 4$) are shown in Fig. 4. Detailed structure in the giant resonance is clearly visible at 15.5, 17.2, 17.9, 19.1, 19.7, 20.8, 21.4, and 22.4 MeV excitation energy while less pronounced structure can be observed at 15.9, 16.3, 18.4, and 20.5 MeV.

Our ground state angular cross section at 90° is compared in Fig. 5 with the one resulting from the electroproton experiment of Tsubota *et al.*⁷ and the one obtained by detailed balance from (p,γ_0) data by Cameron *et al.*⁸ The correspondence with respect to the observed structure is striking, though the resolution in the (p,γ_0) experiment is clearly superior. Our angular cross section at 90° integrated over excitation energy from 14.6 to 24.8 MeV gives (0.155 ± 0.002) MeV fm² sr⁻¹, while the Sendai⁷ and TUNL (Ref. 8) data over the same integration interval yield (0.183 ± 0.001) and 0.181 MeV fm² sr⁻¹, respectively. Our result is about 15% smaller than the values obtained by Tsubota *et al.* and by Cameron *et al.*

Because the asymmetry parameter $a_1(E)$ is finite in the excitation energy interval studied, one can conclude that there is interference between $E1$ and $M1$ or $E2$ absorption. The anisotropy parameter $a_2(E)$ is negative over the

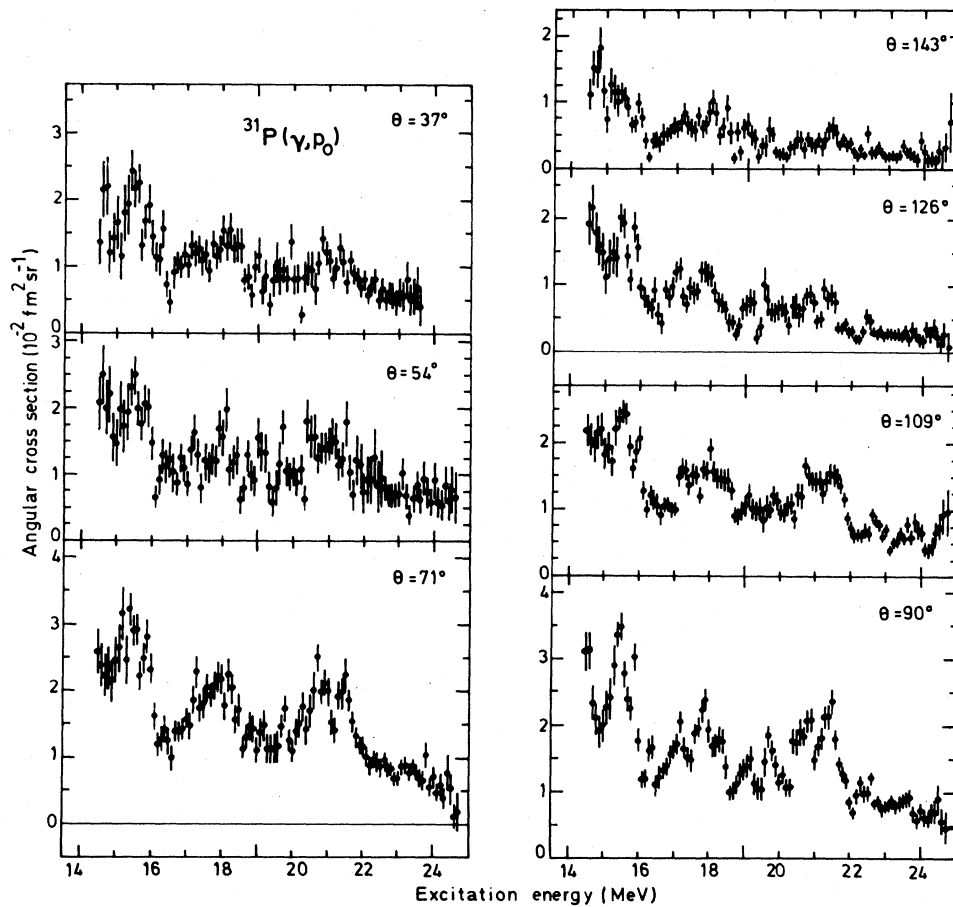


FIG. 2. Angular cross sections for the reaction $^{31}\text{P}(\gamma, p_0)^{30}\text{Si}$ at the seven emission angles θ in the laboratory system, as a function of the excitation energy.

entire range and equals about -0.5 ; this indicates a maximum in the angular dependence of the cross section around 90° . The other asymmetry parameter $a_3(E)$ fluctuates around zero, while the angular factor $a_4(E)$ is positive, which assures the presence of $E2$ absorption, as will be discussed in detail in Sec. III E.

Our (γ, p_0) cross section integrated over excitation energy from 14.6 to 24.8 MeV yields a value of (1.35 ± 0.01) MeV fm 2 . Compared with the over-energy-integrated total photoproton cross section, as obtained in Sec. III D, the ground-state reaction channel contributes only $(6.8 \pm 0.1)\%$ to the total (γ, p) reaction in the corresponding energy region. A similar percentage of $(5.0 \pm 0.5)\%$ was found in the case of the $^{32}\text{S}(\gamma, p)^{31}\text{P}$ reaction 15 with formation of the ^{31}P nucleus in the ground state.

B. The $^{31}\text{P}(\gamma, p_1)$ cross section

The integrated-over-angles (γ, p_1) cross section, derived using the procedure described in Sec. II, is shown in Fig. 6, together with its $a_1(E)$ and $a_2(E)$ angular distribution factors. The absolute magnitude of the cross section is

comparable to that of the (γ, p_0) reaction. Although the statistical accuracy of the data is limited, gross structure is to be seen around 21 MeV. This resonance tends to coincide with a peak identified in the (γ, p_0) cross section.

In Fig. 7 our angular cross section $d\sigma/d\Omega$ at 90° for the (γ, p_1) reaction is compared with the results of Tsubota *et al.* 7 and shows a reasonable agreement. The present angular cross section at 90° , integrated over excitation energy from 16.8 to 24.8 MeV, amounts to (0.097 ± 0.006) MeV fm 2 sr $^{-1}$, while the Sendai data 7 over the same integration interval yields (0.078 ± 0.004) MeV fm 2 sr $^{-1}$. The value of Tsubota *et al.* is now some 20% smaller than ours. In the case of the nucleus ^{27}Al , similar deviations from the Sendai values have been observed by the Moscow group. 3

The (γ, p_1) cross section integrated over excitation energy from 16.8 to 24.8 MeV yields a value of (1.13 ± 0.04) MeV fm 2 . This reaction channel contributes about $(6.0 \pm 0.2)\%$ to the total (γ, p) reaction, i.e., of the same order of magnitude as the ground state channel.

Although the asymmetry factor $a_1(E)$ fluctuates around zero (see Fig. 6), its average value is nonzero ($\langle a_1 \rangle = 0.15 \pm 0.04$), and illustrates the interference be-

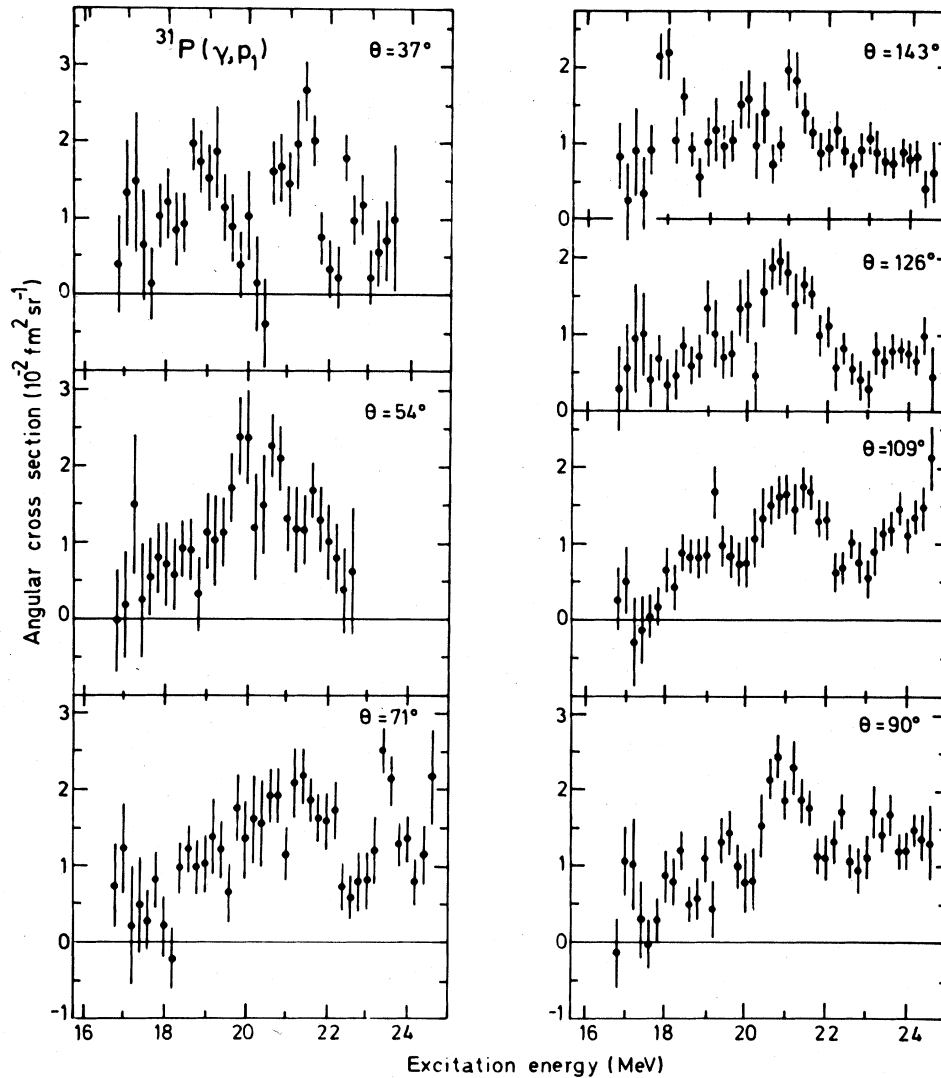


FIG. 3. Angular cross sections for the reaction $^{31}\text{P}(\gamma, p_1)^{30}\text{Si}$ at the seven laboratory observation angles θ as a function of the excitation energy.

tween states of opposite parity. The anisotropy factor $a_2(E)$, which shows large statistical errors, also fluctuates around zero ($\langle a_2 \rangle = -0.01 \pm 0.06$), except around 18 MeV excitation energy. Even if one makes the assumption that only $E1$ and $E2$ photon absorption takes place, a detailed analysis of these factors is impossible as the relations between the angular distribution factors and the multipole matrix elements for this proton channel are too complicated to allow unambiguous conclusions.

C. Branching to the various residual states

The nature of the residual nuclear state determines to a large extent the decay mechanism by which this state can be reached. The excited states of the residual nucleus ^{30}Si

have been well studied both experimentally^{16–18} and theoretically.^{17,19} In an investigation¹⁸ by means of the proton pickup reaction $^{31}\text{P}(d, h)^{30}\text{Si}$ at high bombarding energy, eighteen proton-hole states were identified up to 11.4 MeV. They are listed in Table I together with the available spectroscopic information. All the presently known low-lying levels¹⁶ in ^{30}Si are depicted in Fig. 8(d) and 11 of the resolved proton-hole states¹⁸ (those below 7.1 MeV excitation energy) are shown separately with their spectroscopic strengths in Fig. 8(e). The ground state and two excited states (3.79 and 5.38 MeV) are populated by $l=0$ transfer. The angular distributions referring to all other transitions show an $l=2$ structure. The (γ, p_1) reaction cross sections whereby those proton-hole states in the residual nucleus ^{30}Si are reached may be caused by a direct-semidirect (DSD) reaction mechanism.

In Figs. 8(a)–(c) three examples of integrated-over-

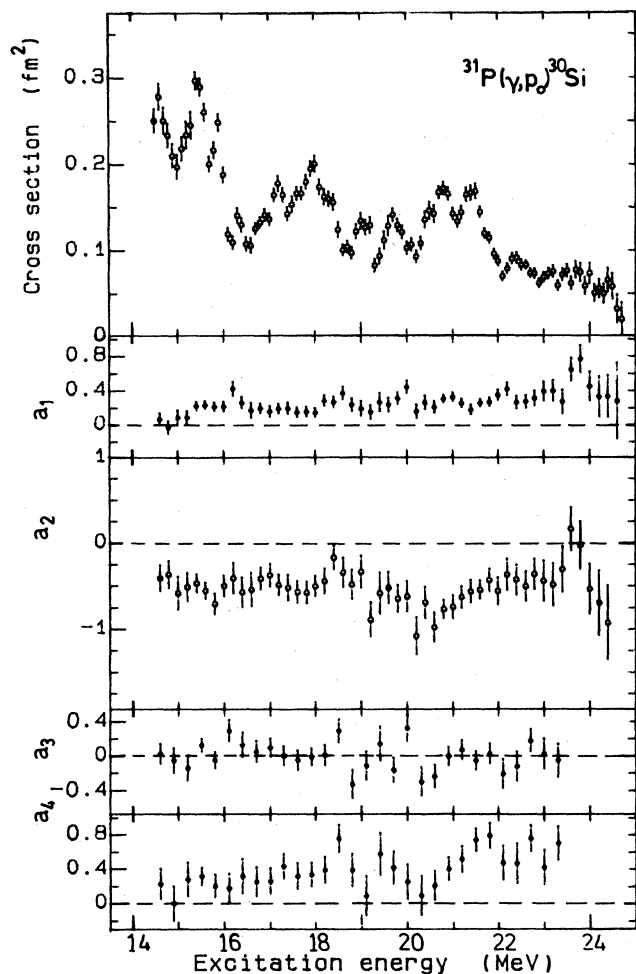


FIG. 4. Cross section and angular distribution factors a_ν ($\nu=1, \dots, 4$) for the reaction $^{31}\text{P}(\gamma, p)^{30}\text{Si}$ as a function of excitation energy.

angles photoproton spectral cross sections $d\sigma/dE_{k,p}$, corresponding to pseudo-monochromatic photon spectra peaking around 18, 21, and 24 MeV, are plotted. As can be seen from these figures, the residual states or groups of states populated by the $^{31}\text{P}(\gamma, p)^{30}\text{Si}$ reaction are effectively located at 0, 2.24, 3.6 (almost the centroid energy for the states at 3.498 and 3.787 MeV), 5.2 (the centroid energy for the states at 4.809, 4.830, 5.230, 5.372, and 5.613 MeV), and 6.9 (the centroid energy for the states at 6.537, 6.865, and 7.079 MeV) MeV. The different members in those groups of states cannot be separated in our experimental results due to the limited energy resolution, which is mainly determined by the width of about 1 MeV of the pseudo-monoenergetic photon flux.

The absolute photoproton cross section for decay to the ground state, to the first excited state, and to the groups of "second," "third," and "fourth" excited states, obtained via both analysis methods described in Sec. II, are displayed in Fig. 9. As can be seen in the figure, there exists nice agreement between the results (experimental

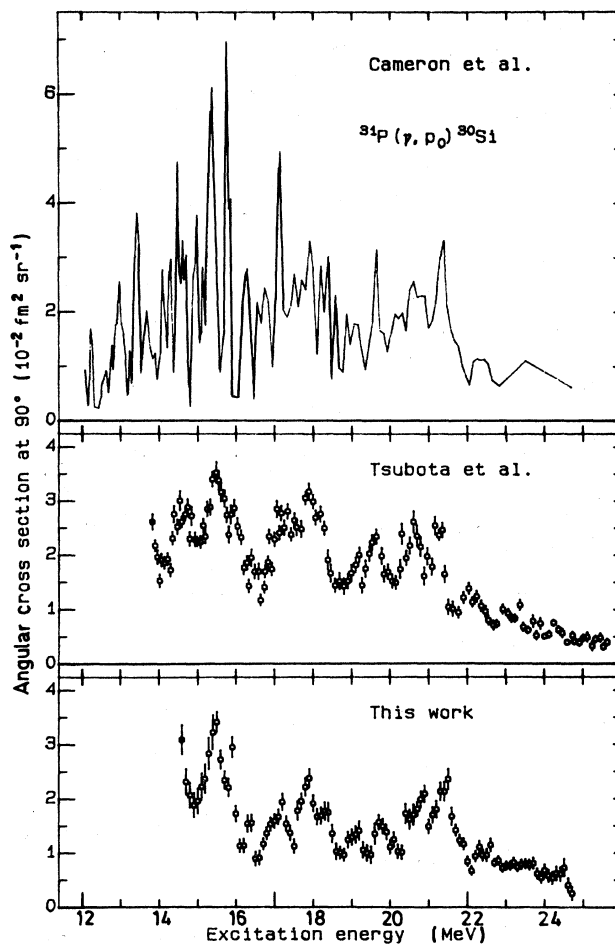


FIG. 5. Comparison between the $^{31}\text{P}(\gamma, p_0)$ angular cross section at the emission angle of 90° vs excitation energy as observed by Cameron *et al.* (Ref. 8), Tsubota *et al.* (Ref. 7), and in this work.

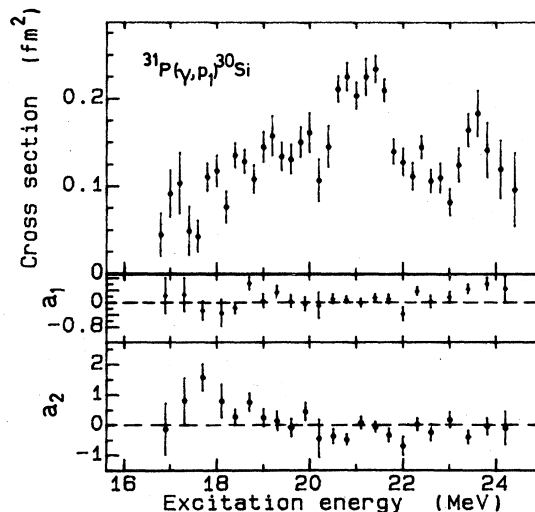


FIG. 6. The $^{31}\text{P}(\gamma, p_1)^{30}\text{Si}$ cross section and angular distribution factors a_ν ($\nu=1, 2$) as a function of excitation energy.

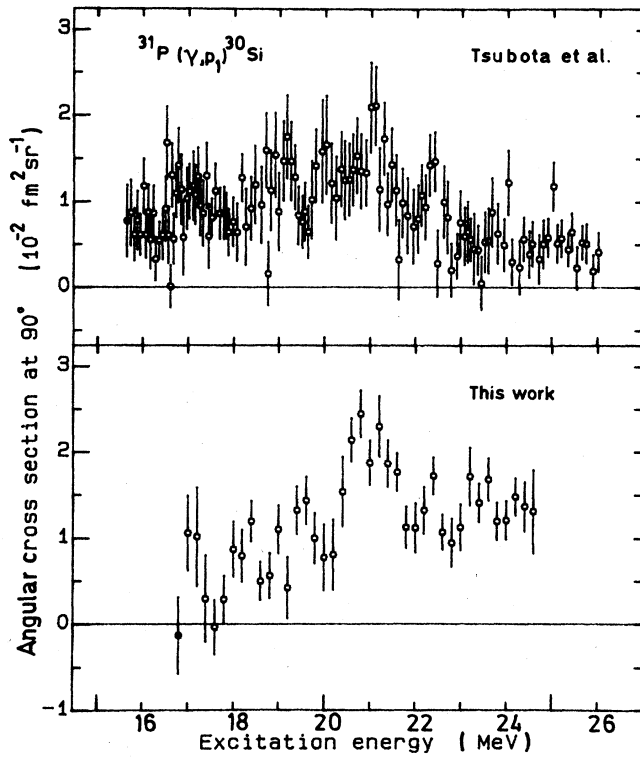


FIG. 7. Comparison between the $^{31}\text{P}(\gamma, p_1)^{30}\text{Si}$ angular cross section at 90° vs excitation energy, measured by Tsubota *et al.* (Ref. 7) and the one observed in the present work.

points) obtained from the artificial pseudo-monoenergetic photon-flux method and those (histograms) produced by the subtraction or peeling off procedure. This branching to the various final states is presented in an alternative way in Fig. 10. The (γ, p_0) cross section and the pseudo-ground-state (γ, p) cross section contributions for decay to the identified residual excited "states," calculated from the results of Fig. 9, are plotted, for the nine different end point energy situations, as histograms. The measured pseudo-ground-state cross sections (i.e., photoproton spectra analyzed to a cross section as if all detected protons would decay to the final ground state) are represented by the data points.

In Table I we compare the absolute combined spectroscopic factors $\sum C^2S$, determined experimentally by Mackh *et al.*,¹⁸ with the integrated values of the presently measured partial cross sections $\int \sigma_{(\gamma, p_i)}(E)dE$ for the $^{31}\text{P}(\gamma, p_i)$ reaction to the same residual "states." Table I indicates the existence of a strong correlation between both quantities of the form

$$\int \sigma_{(\gamma, p_i)}(E)dE = KC^2S(i).$$

Hence one can calculate the proportionality coefficient

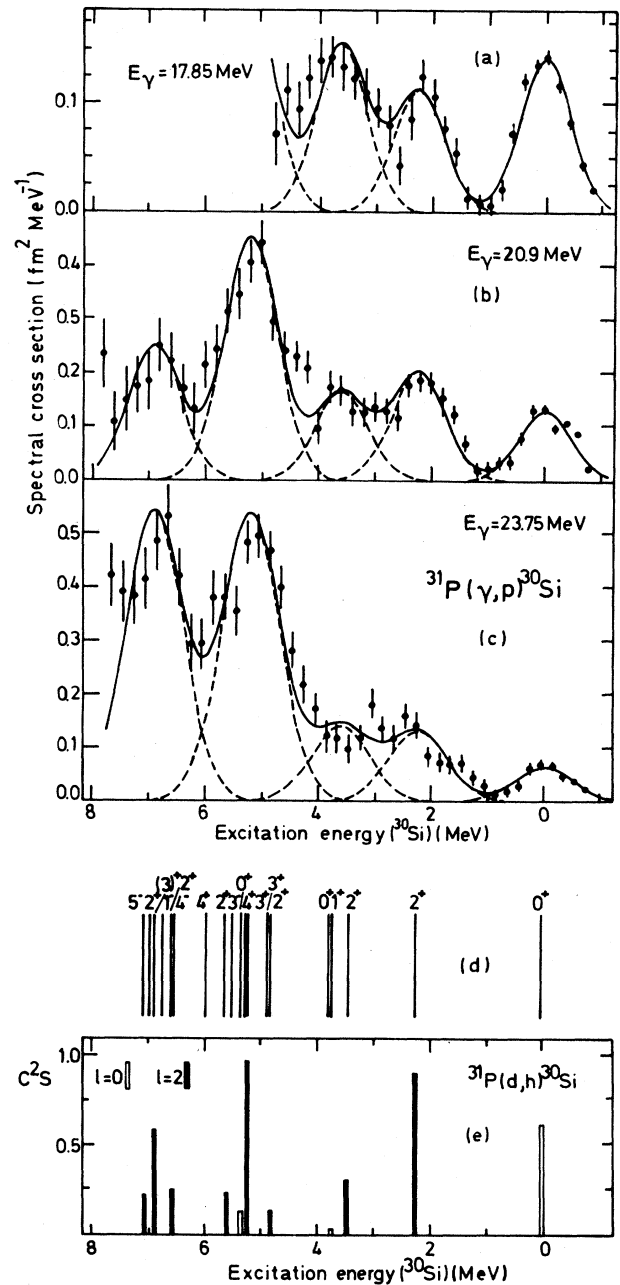


FIG. 8. The ^{31}P photoproton spectral cross section $d\sigma/dE_{k,p}$ vs excitation energy in the final nucleus ^{30}Si , corresponding to pseudo-monoenergetic photon spectra at (a) 17.85, (b) 20.9, and (c) 23.75 MeV; (d) ^{30}Si energy level scheme according to Ref. 16; (e) spectroscopic factors for ^{30}Si proton-hole states as measured by Mackh *et al.* (Ref. 18).

$$K = \frac{\sum_{i=0}^{\text{"4"}} \int \sigma_{(\gamma, p_i)}(E)dE}{\sum_{i=0}^{\text{"4"}} C^2S(i)} \\ = (1.85 \pm 0.03) \text{ MeV fm}^2,$$

while a value of $(2.17 \pm 0.02) \text{ MeV fm}^2$ can be deduced us-

TABLE I. Comparison of the spectroscopic factors (Ref. 18) from the $^{31}\text{P}(d,h)^{30}\text{Si}$ reaction with the integrated values of the partial cross sections as observed in the reactions $^{31}\text{P}(\gamma,p_i)^{30}\text{Si}$.

J^π	$E(^{30}\text{Si})$ (MeV)	nlj	C^2S	$\sum C^2S$	$\int \sigma_{(\gamma,p_i)}(E)dE$ (MeV fm 2)	$\sum_i \int \sigma_{(\gamma,p_i)}dE$ (MeV fm 2)	Label i	Centroid energy (MeV)
0^+	0.00	$2s_{1/2}$	0.62	0.62	1.35 ± 0.01	8.16 ± 0.15	0	0.0
2^+	2.23	$1d_{5/2} + 1d_{3/2}$	$0.34 + 0.57$	0.91	1.13 ± 0.04		1	2.24
2^+	3.51	$1d_{5/2} + 1d_{3/2}$	$0.27 + 0.04$	0.34	0.97 ± 0.05		"2"	3.6
0^+	3.79	$2s_{1/2}$	0.03					
3^+	4.84	$1d_{5/2} + 1d_{3/2}$	$0.13 + 0.01$	4.42	2.88 ± 0.09	"3"	5.2	
3^+	5.24	$1d_{5/2}$	0.98					
0^+	5.38	$2s_{1/2}$	0.14					
2^+	5.62	$1d_{5/2}$	0.23					
2^+	6.55	$1d_{5/2}$	0.25	1.06	1.83 ± 0.10	(10.5)	"4"	6.9
$(3)^+$	6.87	$1d_{5/2}$	0.59					
$(1,3)^+$	7.08	$1d_{5/2}$	0.22					
2^+	7.26	$1d_{5/2}$	0.12	1.29		(2.4)		
0^+	7.44	$1d_{5/2}$	0.06					
	7.66	$1d_{5/2}$	0.37					
	8.14	$1d_{5/2}$	0.27					
	8.78	$1d_{5/2}$	0.14					
	8.92	$1d_{5/2}$	0.15					
	9.24	$1d_{5/2}$	0.18					

ing the ground state data only. A similar analysis was performed recently in the case of a (p,γ_i) investigation by Snover.²⁰ Summation of the absolute spectroscopic factors for the seven proton-hole states¹⁸ higher than 7.1 MeV amounts to 1.29 (see Table I). Assuming that the above-mentioned proportionality coefficient applies to the higher proton-hole states as well, the integrated (γ,p) cross section leading to those states would amount to 2.4 MeV fm 2 . We can now estimate the contribution of the direct-semidirect and of the statistical reaction mechanisms. The sum of the energy-integrated photoproton cross sections in the 14.6 to 23.9 MeV excitation energy region, populating all the proton-hole states in the final nucleus ^{30}Si up to an excitation energy of about 11.4 MeV, amounts to 10.5 MeV fm 2 . The energy-integrated total photoproton cross section, obtained by the Thies unfolding technique (see Sec. III D), in the same excitation energy region yields (19.8 ± 0.1) MeV fm 2 . Hence¹² it seems reasonable to conclude that some 53% of the protons are emitted by a direct-semidirect process and that the remaining part is caused by a statistical or preequilibrium reaction mechanism.

D. The total $^{31}\text{P}(\gamma,p)$ cross section

The total photoproton cross section $\sigma(\gamma,p)$ for ^{31}P was derived from the total photoproton yield as explained in Sec. II. The result, shown in Fig. 11, was obtained with an analysis interval of 2 MeV, which gives rise to the (quite large) horizontal resolution bars.

Ishkhanov *et al.*²¹ studied the $^{31}\text{P}(\gamma,p)$ cross section in

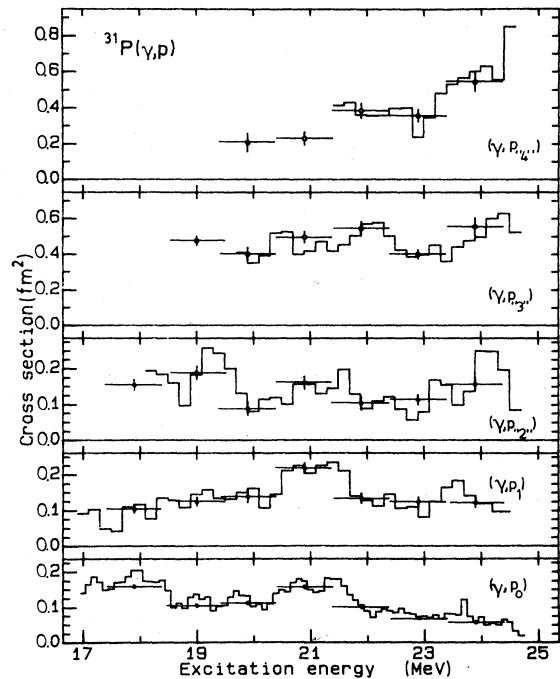


FIG. 9. The absolute cross sections for the $^{31}\text{P}(\gamma,p_i)$ reaction ($i=0, \dots, "4"$) leading to the ground state, first excited state, and groups of states at 3.6, 5.2, and 6.9 MeV in ^{30}Si as a function of excitation energy; points with error bars according to the pseudo-monoenergetic photon-flux method and histograms obtained by using the peeling off procedure.

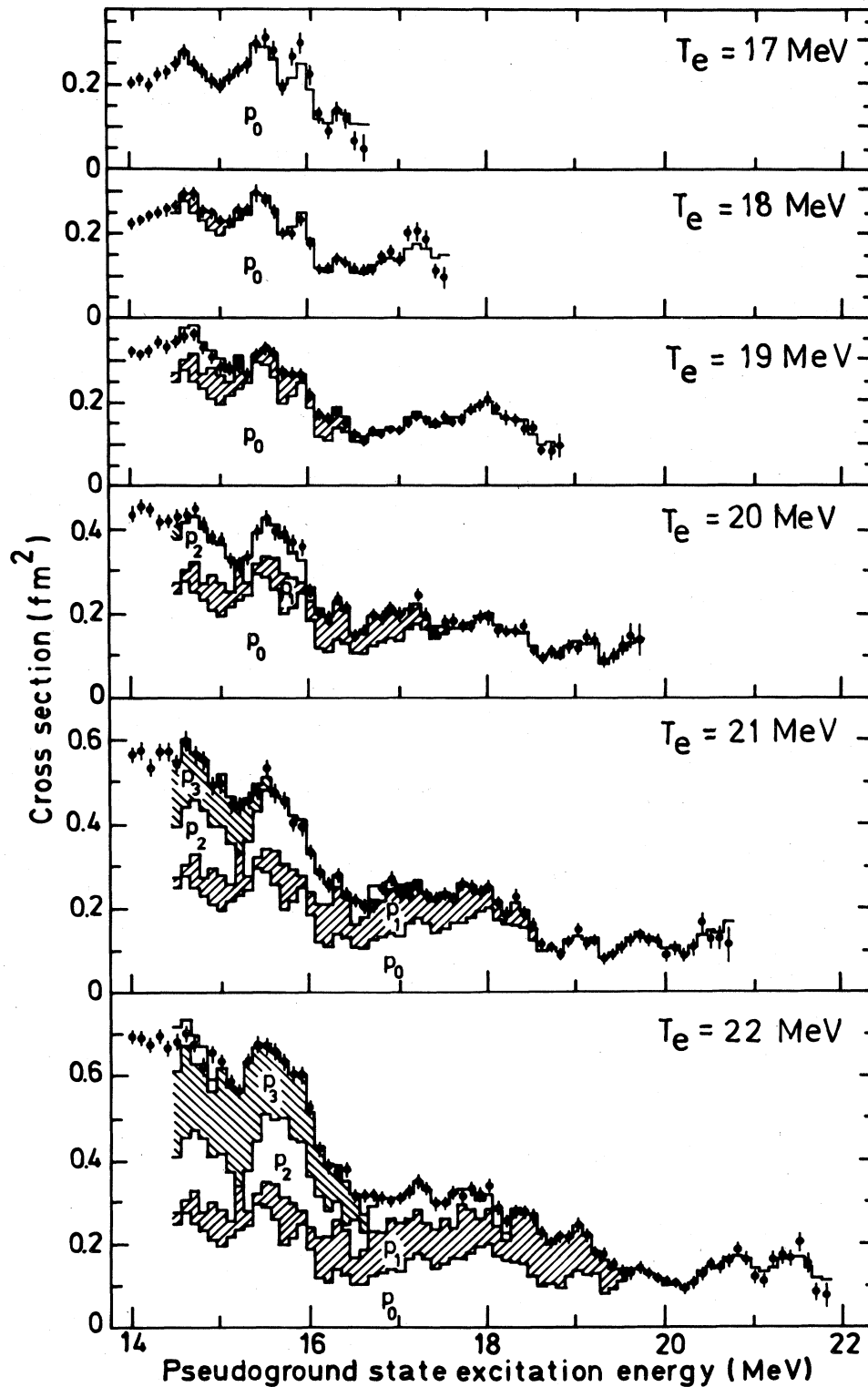


FIG. 10. The ^{31}P pseudo-ground-state photoproton cross section, obtained experimentally (dots with error bars) at the different bremsstrahlung end point energies of this work and its decomposition (histograms) into the contributions leading to different final states or groups of states in ^{30}Si , as a function of the pseudo-ground-state excitation energy.

the excitation energy region from 16 to 32 MeV by measuring with scintillation counters the photoproton yield at a 35 MeV betatron (see also Fig. 11). They found a maximum cross section of about 4.2 fm^2 at 22 MeV, compared to a value of 2.9 fm^2 for our measurement at the same energy. Both their and our cross section curves exhibit a slight indication of a shoulder on the peak at 19

MeV. Their total cross section integrated over energy from threshold up to 32 MeV is equal to $(35 \pm 6) \text{ MeV fm}^2$. Although we find in the rising side of the $^{31}\text{P}(\gamma, p)$ cross section integrated up to 24 MeV almost the same strength as in the corresponding part of the measurement by Ishkhanov *et al.*, our results represent a far less steep leading edge in the cross section than theirs.

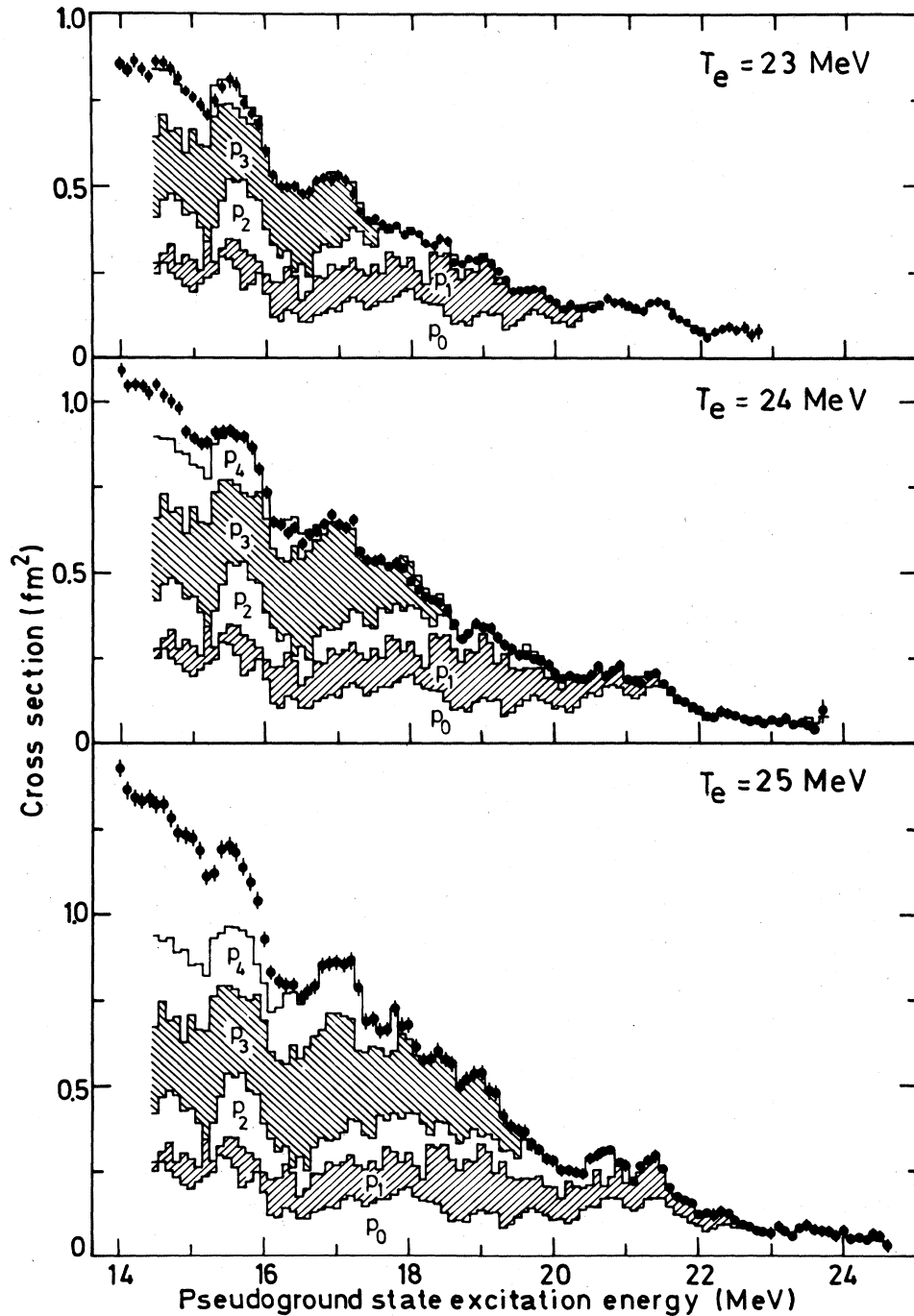


FIG. 10. (Continued).

The energy-integrated total photoneutron cross section

$$\sigma_0 = \int_0^{29 \text{ MeV}} \sigma_{(\gamma, n_{\text{tot}})}(E) dE$$

obtained by Veysière *et al.*⁶ for ^{31}P yields (18.2 ± 1.2) MeV fm^2 . The Thomas-Reiche-Kuhn (TRK) classical sum rule for the energy-integrated photonuclear dipole cross section $6NZ/A \text{ MeV fm}^2$ is equal to 46.5 MeV fm^2 in the case of ^{31}P . Hence the (γ, n_{tot}) channel would represent 39% of this value, while Ishkhanov's (γ, p) measurement would cover 75% of it; the sum of both [which includes twice some 5 MeV fm^2 , i.e., about 10%, due to double counting⁶ of the (γ, pn) process present in both measurements] would slightly exceed the classical sum rule value.

E. Estimate of the $E2$ contribution in the (γ, p_0) reaction channel

For the excitation energy interval under consideration, it is reasonable to take only (coherent) $E1$ and $E2$ photon absorption processes into account (see Fig. 1), since the $M1$ magnetic dipole resonance is expected²² to have its maximum strength around 13 MeV. With this limitation, in the channel spin formalism, the (normalized) angular distribution factors a are related to the transition matrix elements by²³

$$1 = p_{1/2}^2 + 2p_{3/2}^2 + 2d_{3/2}^2 + 3d_{5/2}^2 \quad (\text{normalization}),$$

$$a_1 = 2\sqrt{3}p_{1/2}d_{3/2}\cos(p_{1/2}, d_{3/2}) + \frac{18\sqrt{3}}{5}p_{3/2}d_{5/2}\cos(p_{3/2}, d_{5/2}) + \frac{2\sqrt{3}}{5}p_{3/2}d_{3/2}\cos(p_{3/2}, d_{3/2}),$$

$$a_2 = -p_{3/2}^2 + d_{3/2}^2 + \frac{12}{7}d_{5/2}^2 - 2p_{1/2}p_{3/2}\cos(p_{1/2}, p_{3/2}) + \frac{6}{7}d_{3/2}d_{5/2}\cos(d_{3/2}, d_{5/2}),$$

$$a_3 = -\frac{8\sqrt{3}}{5}p_{3/2}d_{5/2}\cos(p_{3/2}, d_{5/2}) - 2\sqrt{3}p_{1/2}d_{5/2}\cos(p_{1/2}, d_{5/2}) - \frac{12\sqrt{3}}{5}p_{3/2}d_{3/2}\cos(p_{3/2}, d_{3/2}),$$

$$a_4 = -\frac{12}{7}d_{5/2}^2 - \frac{48}{7}d_{3/2}d_{5/2}\cos(d_{3/2}, d_{5/2}).$$

This represents a set of five quadratic equations with seven unknowns. These unknowns are the four moduli $p_{1/2}$, $p_{3/2}$, $d_{3/2}$, and $d_{5/2}$ of the reaction matrix elements and the three phase differences $(p_{1/2}, d_{3/2})$, $(p_{3/2}, d_{3/2})$, and $(p_{3/2}, d_{5/2})$. Indeed the $\frac{1}{2}^+$ ground state of ^{31}P is connected (see Fig. 1) with the two $\frac{1}{2}^-$ and $\frac{3}{2}^-$ dipole

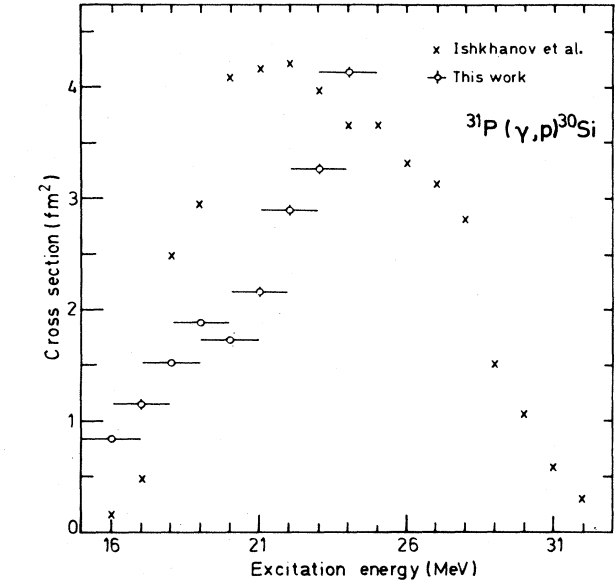


FIG. 11. The total $^{31}\text{P}(\gamma, p)^{30}\text{Si}$ cross section as a function of excitation energy as measured by Ishkhanov *et al.* (Ref. 21) (crosses) and as obtained in this experiment (points and error bars).

channels (with subsequent $p_{1/2}$ wave emission and $p_{3/2}$ wave emission) and with the two $\frac{3}{2}^+$ and $\frac{5}{2}^+$ quadrupole channels (subsequent $d_{3/2}$ wave emission and $d_{5/2}$ wave emission). Since one phase can be chosen arbitrarily, the differences between the corresponding phases can be symbolized by, e.g., $(p_{1/2}, d_{3/2}) = \phi_{p_{1/2}} - \phi_{d_{3/2}}$.

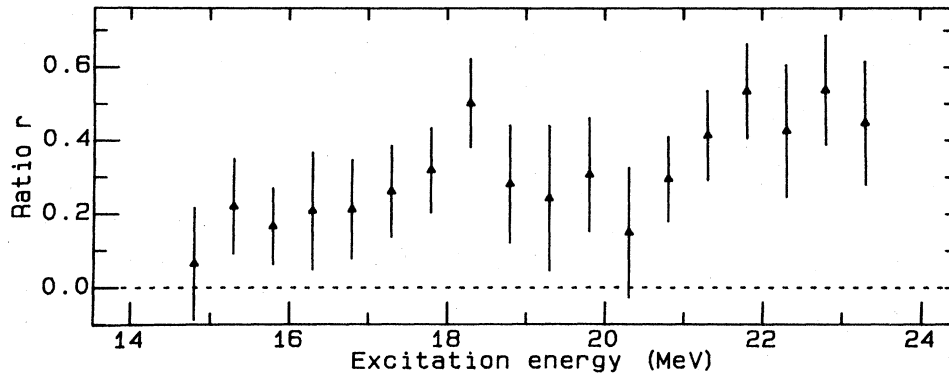


FIG. 12. The ratio $r(E)$ of the minimum $E2$ to the total ^{31}P photoproton ground state cross section versus excitation energy E .

The preceding set of equations cannot be solved without additional assumptions. We will therefore restrict the discussion to the minimum $E2$ contribution to the (γ, p_0) cross section, which can be derived unambiguously. The ratio $r(E)$ of the quadrupole to the total (γ, p_0) cross section, defined as

$$r(E) = \sigma^{E2}(E) / [\sigma^{E1}(E) + \sigma^{E2}(E)] \\ = 2d_{3/2}^2 + 3d_{5/2}^2,$$

can be minimized in a straightforward way, leading to $r_{\min}(E) = +(7/8)a_4$ if $a_4 \geq 0$ and $r_{\min}(E) = -(7/12)a_4$ if $a_4 \leq 0$. This result is displayed in Fig. 12. Note that our experimental a_4 values are positive over the entire energy interval studied (see Fig. 4), in poor agreement with the results of Cameron *et al.*⁸

However, we wish to point out here that we can tentatively solve the full set of equations after reducing the number of unknowns on reasonable grounds. We have explored two different approaches: either assuming that $(p_{1/2}, p_{3/2}) = n\pi$ and $(d_{3/2}, d_{5/2}) = m\pi$ (with $n, m \in \mathbf{N}_0$), or assuming that $p_{1/2} = p_{3/2}$ and $d_{3/2} = d_{5/2}$; incidentally, both are compatible with the results of a DSD calculation.⁸ Each approximation leads to nearly the same estimated $E2$ cross section magnitude, only slightly different from the minimum value.

In Fig. 13 we compare our minimum $E2$ cross section with the preferred $E2$ solution of Cameron *et al.*,⁸ and with the results of a DSD-model calculation.⁸ In Cameron's experiment a polarized proton capture measurement on ^{30}Si was performed. Expansion of their measured angular distributions of the analyzing powers in a series of associated Legendre polynomials leads to a set of b_ν factors, which are also related to the reaction matrix elements. In considering only $E1$ and $E2$ radiation, they

were able to construct a system of nine equations relating their measured a_ν and b_ν factors ($\nu=1, \dots, 4$) with the seven basic unknowns (four moduli and three phase differences) mentioned earlier in this section. Calculations based on a simple and on an extended direct-semidirect capture model indicated that their solution set II is the physical one.

As the isovector $E2$ resonance would probably²² be centered around 31 MeV (which is out of the energy range we consider here), we only have to take into account the isoscalar component. The energy weighted sum rule (EWSR) for the $E2$ cross section is given, in the case of $\Delta T=0$ transitions, by

$$\int \frac{\sigma^{E2}}{E^2} dE = \frac{\alpha\pi^2}{3} \frac{\langle r^2 \rangle}{m_p c^2} \frac{Z^2}{A},$$

with α the fine structure constant; for ^{31}P with $\sqrt{\langle r^2 \rangle} = 3.19$ fm,²⁴ the value of the EWSR is 1.89×10^{-3} fm² MeV⁻¹. Our experimental value of the integral $\int \sigma^{E2} E^{-2} dE$ from $E=14.6$ to 23.5 MeV is $(1.05 \pm 0.15) \times 10^{-3}$ fm² MeV⁻¹ for the minimum solution; this would indicate that the (γ, p_0) channel exhausts at least 48% of the $(\Delta T=0)$ $E2$ EWSR. This value is quite high, and should be referred to with some caution, as it is solely based on the a_4 factor, which might be overestimated by maximum 25% due to small asymmetries in the detector setup. The experimental data of Cameron *et al.* for $E=12.9$ to 21.9 MeV, analyzed following solution set II, would only take up $(0.60 \pm 0.05) \times 10^{-3}$ fm² MeV⁻¹, while the prediction of the extended DSD-model calculation is still an order of magnitude smaller, i.e., 0.045×10^{-3} fm² MeV⁻¹.

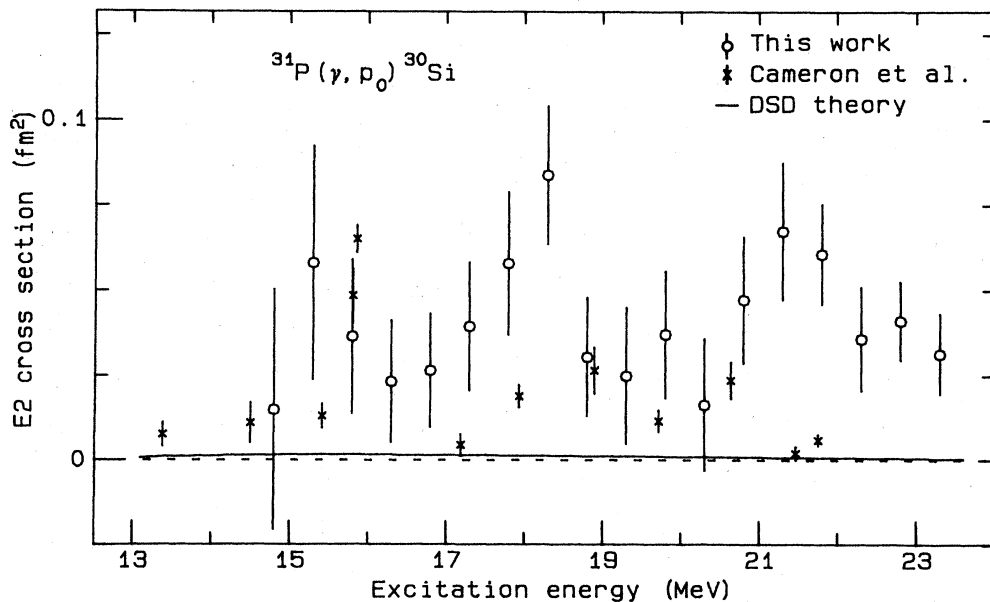


FIG. 13. The $E2$ cross section for the $^{31}\text{P}(\gamma, p_0)^{30}\text{Si}$ reaction, according to Cameron *et al.* (Ref. 8) (crosses) and its minimum magnitude deduced from this work (dots); the solid line is the extended DSD prediction.

IV. CONCLUSIONS

The $^{31}\text{P}(\gamma, p_0)^{30}\text{Si}$ and $^{31}\text{P}(\gamma, p_1)^{30}\text{Si}$ reaction cross sections and angular distributions have been studied in an absolute way with bremsstrahlung photons over a large part (excitation energy region from 14.6 to 25.0 MeV) of the giant dipole resonance. Agreement with earlier alternative measurements is fair. While both reaction channels mentioned each contribute less than 10% to the total photoproton reaction, stronger decay to groups of low-lying states has been observed. Good correlation was found between these results and combined proton-pickup spectroscopic factors. The total (γ, p) reaction cross section was determined in the rising part of the GDR. It does not show that steep slope as was suggested by Ishkhanov *et al.* In the excitation energy region studied, about half of this cross section would be caused by a direct-semidirect reaction mechanism. In the (γ, p_0) channel an

$E2$ cross section was deduced exhausting at least 48% of the isoscalar quadrupole energy-weighted sum rule.

ACKNOWLEDGMENTS

We wish to thank Prof. A. J. Deruytter for his interest in this work. We are especially grateful to the linac crew for the operation of the linear accelerator and to the technical and administrative staff of our laboratory for their help. One of us (A.A.) would like to thank the Ministry of Education, Republic of Turkey; the Ministerie van Nationale Opvoeding en Nederlandse Cultuur, Belgium; and the Rijksuniversiteit Gent, Belgium for fellowships, which enabled him to carry out his research work in Ghent. We also acknowledge the financial support lent by the Interuniversity Institute for Nuclear Sciences (IIKW) and the National Fund for Scientific Research (NFWO), Brussels, Belgium.

*Present address: Laboratorium voor Natuurkunde II, Rijksuniversiteit Gent, B-9000 Gent, Belgium.

¹B. L. Berman and S. C. Fultz, *Rev. Mod. Phys.* **47**, 713 (1975).

²E. Kerkhove, H. Ferdinande, R. Van de Vyver, P. Berkvens, P. Van Otten, E. Van Camp, and D. Ryckbosch, *Phys. Rev. C* **29**, 2047 (1984); E. Kerkhove, Ph.D. thesis, Rijksuniversiteit, Gent (unpublished).

³B. S. Ishkhanov, I. M. Kapitonov, V. I. Shvedunov, and A. V. Shumakov, *Yad. Fiz.* **33**, 865 (1981) [*Sov. J. Nucl. Phys.* **33**, 453 (1981)].

⁴P. J. P. Ryan, M. N. Thompson, K. Shoda, and T. Tanaka, *Nucl. Phys.* **A371**, 318 (1981); P. J. P. Ryan, M. N. Thompson, K. Shoda, and M. Hirooka, *ibid.* **A389**, 29 (1982).

⁵J. Devos, R. Carchon, H. Ferdinande, and R. Van de Vyver, *Z. Phys.* **271**, 391 (1974), and references therein.

⁶A. Veyssière, H. Beil, R. Bergère, P. Carlos, A. Leprêtre, and A. De Miniac, *Nucl. Phys.* **A227**, 513 (1974).

⁷H. Tsubota, N. Kawamura, S. Oikawa, M. Sugawara, and K. Shoda, *J. Phys. Soc. Jpn.* **35**, 330 (1973), and references therein.

⁸C. P. Cameron, R. D. Ledford, M. Potokar, D. G. Rickel, N. R. Roberson, H. R. Weller, and D. R. Tilley, *Phys. Rev. C* **22**, 397 (1980).

⁹B. J. Thomas, A. Buchnea, J. D. Irish, and K. G. McNeill, *Can. J. Phys.* **50**, 3085 (1972); M. N. Thompson, private communication.

¹⁰R. Carchon, R. Van de Vyver, H. Ferdinande, J. Devos, and E. Van Camp, *Phys. Rev. C* **14**, 456 (1976).

¹¹E. Van Camp, R. Van de Vyver, H. Ferdinande, E. Kerkhove, R. Carchon, and J. Devos, *Phys. Rev. C* **22**, 2396 (1980).

¹²E. Van Camp, R. Van de Vyver, E. Kerkhove, D. Ryckbosch,

H. Ferdinande, P. Van Otten, and P. Berkvens, *Phys. Rev. C* **24**, 2499 (1981).

¹³D. Ryckbosch, E. Van Camp, R. Van de Vyver, E. Kerkhove, P. Van Otten, P. Berkvens, and H. Ferdinande, *Phys. Rev. C* **26**, 448 (1982).

¹⁴D. M. Crawford, R. Koch, and H. H. Thies, *Nucl. Instrum. Methods* **109**, 573 (1973).

¹⁵V. V. Varlamov, B. S. Ishkhanov, I. M. Kapitonov, Z. L. Kocharova, V. N. Orlin, and V. I. Shvedunov, *Izv. Akad. Nauk SSSR, Ser. Fiz.* **42**, 153 (1978) [*Bull. Acad. Sci. USSR, Phys. Ser.* **42**, 132 (1978)].

¹⁶P. Endt and C. Van der Leun, *Nucl. Phys.* **A310**, 1 (1978).

¹⁷B. H. Wildenthal and E. Newman, *Phys. Lett.* **28B**, 108 (1968).

¹⁸H. Mackh, G. Mairle, and G. J. Wagner, *Z. Phys.* **269**, 353 (1974).

¹⁹M. J. A. De Voigt and B. H. Wildenthal, *Nucl. Phys.* **A206**, 305 (1973); B. H. Wildenthal and J. B. McGrory, *Phys. Rev. C* **7**, 714 (1973); B. H. Wildenthal, J. B. McGrory, E. C. Halbert, and D. H. Graber, *ibid.* **4**, 1708 (1971).

²⁰D. H. Dowell, G. Feldman, K. A. Snover, A. M. Sandorfi, and M. T. Collins, *Phys. Rev. Lett.* **50**, 1191 (1983); K. A. Snover, *Bull. Am. Phys. Soc.* **28**, 651 (1983).

²¹B. S. Ishkhanov, I. M. Kapitonov, V. G. Shevchenko, and B. A. Yur'ev, *Phys. Lett.* **9**, 162 (1964).

²²F. E. Bertrand, *Annu. Rev. Nucl. Sci.* **26**, 457 (1976).

²³R. W. Carr and J. E. E. Baglin, *Nucl. Data Tables* **A10**, 143 (1971).

²⁴C. W. de Jager, H. de Vries, and C. de Vries, *At. Data Nucl. Data Tables* **14**, 479 (1974).